To be or not to be a SNA: That is the question

Àlex Haro and Carles Simó

Dept. de Matemàtica Aplicada i Anàlisi, Universitat de Barcelona,

Gran Via 585, Barcelona 08007, SPAIN *

Abstract

We study the phenomenon of transition to chaos in quasiperiodically forced dissipative dynamical systems. In particular, we study the so called fractalization route, in which a smooth torus seems to fractalize. This has been suggested by several authors as a scenario of formation of strange nonchaotic attractors. We provide numerical evidence, supported in rigorous results, that some of these attractors are really non-strange.

PACS numbers: 05.45.-a 05.45.Df 47.52.+j 47.53.+n

The study of the transition from order to chaos is one of the central strands of Nonlinear Science, and has attracted the attention of a number of scientists of different areas. In particular, in the study of dissipative dynamical systems the notion of *Strange Attractor* [1] is one of the most important.

Attractors are relevant because they are visible invariant sets of the dynamics. An *attractor* $\mathcal{A}$ is an object that traps the motion of a set of positive measure. If $\mathcal{A}$ is geometrically complex, say it is not a (piecewise) smooth manifold, we say that it is *strange*. If orbits on $\mathcal{A}$ exhibit sensitive dependence on initial conditions [2] we say that it is *chaotic*. While the first examples of strange attractors were *Strange Chaotic Attractors* (SCA for short), Grebogi et al. [3] suggested the existence of *Strange Nonchaotic Attractors* (SNA for short) in two models. Since then SNAs have been observed in many others [4]. Besides numerical observations, they have been proved to exist rigorously in some cases [5–11]. But, as we will see, not everything which is believed to be a SNA really is [12–14].

In this Letter, we consider dissipative systems in which there is a quasiperiodic (qp for short) forcing [30]. Hence the transition from regular to chaotic dynamics is described as the bifurcation from an attracting invariant curve (or 1D torus) to a SCA. In the literature, it has been proposed a scenario in which a mixture of both kinds of dynamics appears in the interplay, geometrically described as the creation of a SNA. This is the so called *fractalization route* [15, 16], in which "a qp torus gets increasingly wrinkled and transform into a SNA without the apparent mediation of any nearby unstable periodic orbit" [4]. Our aim is to give further numerical evidence, supported by rigorous results, that *in the fractalization route SNAs are NOT produced*. To reach this conclusion, we have analyzed numerically the fine scale structure of several nonchaotic attractors, suggested to be strange in the literature, discovering that they are really nonstrange. At the end we also provide a theoretical explanation of the phenomenon.

The models we consider are of the form

$$x_{n+1} = f_{a,\varepsilon}(x_n, \theta_n), \quad \theta_{n+1} = \theta_n + \omega \pmod 1, \tag{1}$$

where $x \in \mathbb{R}^N$ are state variables and $\theta \in \mathbb{T} = \mathbb{R}/\mathbb{Z}$ is an angular variable, $a \in \mathbb{R}^P$ and $\varepsilon \in \mathbb{R}$ are parameters (with ε leading to the qp forcing), and ω is an external *frequency* ($\omega \notin \mathbb{Q}$). Thus, (1) is a dynamical system in $\mathbb{R}^N \times \mathbb{T}$ whose evolution from an initial condition (x_0, θ_0) is described by the n-th powers $F^{(n)}_{a,\varepsilon}(x_0, \theta_0) = (f^{(n)}_{a,\varepsilon}(x_0, \theta_0), \theta_0 + n\omega)$.

Given (x_0, θ_0), the dependence on small perturbations of x_0, say v_0, is measured by the Lya-

punov exponent

$$\lambda_{a,\varepsilon}(x_0,\theta_0,v_0)=\lim_{n\to+\infty}\frac{1}{n}\log\left|\mathrm{D}_x f^{(n)}_{a,\varepsilon}(x_0,\theta_0)v_0\right|, \tag{2}$$

where $|\cdot|$ denotes a norm in $\mathbb{R}^N$ [31]. We also define the maximal Lyapunov exponent in the x-direction (λ for short)

$$\lambda_{a,\varepsilon}(x_0,\theta_0)=\max_{v_0\in\mathbb{R}^N\setminus\{0\}}\lambda_{a,\varepsilon}(x_0,\theta_0,v_0). \tag{3}$$

If the orbits on the attractor $\mathcal{A}$ have negative Lyapunov exponents we say it is *nonchaotic* (NA for short).

We consider invariant objects for (1) that carry the qp motion given by ω. An object which could be described as the graph of a map $X=X_{a,\varepsilon}(\theta)$ is invariant under (1) if the *invariance equation*

$$f_{a,\varepsilon}(X_{a,\varepsilon}(\theta),\theta)=X_{a,\varepsilon}(\theta+\omega) \tag{4}$$

holds for all the points on the graph. If $X_{a,\varepsilon}$ is continuous, the object is an invariant curve. If, moreover, it is a NA, then it is as smooth as the system (1) [17, 18].

In this Letter, we focus on the local structure of NA. Many authors measure fractal dimensions and other observables to study the smooth or fractal nature of these attractors. In the following paragraphs, we describe the numerical tools we use.

First of all, to know if an attractor of (1) is NA we estimate $\lambda_{a,\varepsilon}(x_0,\theta_0)$. To do this, we take this (x_0,θ_0) "on" $\mathcal{A}$ (say, we take any point close to $\mathcal{A}$ and iterate a transient time) and a unitary vector v_0, and extend (1) by

$$w_{n+1}=\mathrm{D}_x f(x_n,\theta_n)v_n,\ v_{n+1}=w_{n+1}/|w_{n+1}|. \tag{5}$$

The average slope of the *Lyapunov sums* [12]

$$L_n=\sum_{k=1}^{n}\log|w_k| \tag{6}$$

approaches $\lambda_{a,\varepsilon}(x_0,\theta_0,v_0)$, but taking random v_0 the convergence is almost surely to the maximal Lyapunov exponent: $\lambda=\lim_{n\to\infty}\frac{1}{n}L_n$. Notice that even if $\lambda<0$ and so local errors go to zero, there can be transients in which errors are highly amplified. To measure local irregularities in the behavior of L_n we define the *maximal positive oscillation of the Lyapunov sums* (*mpols* for short) up to step n as

$$P_n=\max_{j\le k\le n}(L_k-L_j)\quad\text{and}\quad P=\lim_{n\to\infty}P_n. \tag{7}$$

To compute accurately points of a NA we proceed as follows. First, we estimate $\lambda < 0$ and P as above. While λ produces an estimate of how long takes a point to go near $\mathcal{A}$, P says that local errors in the iterates can be amplified by $\exp P$. If they exceed the accuracy of the computation all the digits in the iterates can be wrong. So, to do a reliable computation of a point on $\mathcal{A}$, say with d_r decimal digits: (a) we take a large enough transient m with $\exp(m\lambda + P) < 10^{-d_r}$; (b) we use multiprecision arithmetics with d_c digits (MP-d_c for short), with $10^{-d_r} > 10^{-d_c} \exp P$. Hence, for a given θ_0, to estimate the corresponding point in $\mathcal{A}$ we take an arbitrary x_0 and compute $X(\theta_0) \approx f^{(m)}(x_0, \theta_0 - m\omega)$. As checks, new computations are done increasing d_c and m, changing x_0, and comparing the results. Hence, points on $\mathcal{A}$ can be computed in a very reliable way.

The observable we use to study $\mathcal{A}$ at different scales is the (local) variation of $X = X(\theta)$, which we define for $\theta^0 \in \mathbb{T}$, $h > 0$ and $p \in \mathbb{N}$ by

$$V_{h,p}X(\theta^0) = \sum_{i=1}^{p} |X(\theta^i) - X(\theta^{i-1})|,$$

where $\theta^i = \theta^0 + ih$ for $i = 0, \ldots, p$. Heuristically, $V_{h,p}X(\theta^0)$ measures the oscillation of X in the equispaced grid of size p of $[\theta^0, \theta^p]$. The averaged slope of the broken line determined by the nodes $(X(\theta^i), \theta^i)$ is $S_{h,p}X(\theta^0) = \frac{1}{ph} V_{h,p}X(\theta^0)$. If p is fixed and X is smooth, $V_{h,p}X(\theta^0)$ goes to zero with h, but the convergence can be very slow if X is very wild. Moreover, in such a case $S_{h,p}X(\theta^0)$ goes to $|X'(\theta^0)|$.

To study the local structure of $\mathcal{A}$ we make successive zooms, trying to catch up the wilder regions of $\mathcal{A}$. To do so, we fix integers $q >> s > 1$ and, starting from $I_0 = [0, 1]$, we construct nested intervals I_k as follows (*zooming algorithm*):

> Given an interval I_k, we make s subdivisions of equal length, and choose I_{k+1} as the subinterval that has the largest variation in its grid of size q.

Notice that the length of I_k is $\ell_k = s^{-k}$. We also define V_k as the variation in the grid of size $p = sq$ of I_k, and the corresponding averaged slope is $S_k = s^k V_k$. The zooming algorithm produces $I_0 \supset I_1 \supset \ldots \supset I_k \supset \ldots$ with $\ell_k \to 0$. So the intervals go to an unique point. The limit depends on q, s, but for an invariant graph X the properties around one point are translated to the whole graph by the qp motion.

We emphasize that multiprecision is crucial to make a reliable study to very small scales. We have used both PARI package and GMP C-library to compute $\mathcal{A}$ and apply the zooming algorithm.

In the results shown here, the points of the attractors have been computed with more than 30 correct digits.

Lyapunov exponents have a statistical character. So, we use standard double/quadruple precision to compute them, provided that the orbit is accurately computed, we use scaling in (5), we perform several approximations taking different ns, interpolate, etc (see, e.g., [19] and references therein). In all the examples of this paper we have computed λ with more than 5 correct digits, enough to distinguish if $\lambda < 0$ or $\lambda < 0$.

Armed with the described tools, we consider several interesting and elementary qp systems like (1) that have appeared in the literature. In all of them we select $\omega = \frac{\sqrt{5}-1}{2}$.

The first example is a *qp forced logistic map*,

$$\begin{aligned} x_{n+1} &= a x_n (1 - x_n) + \varepsilon \sin(2\pi\theta_n), \\ \theta_{n+1} &= \theta_n + \omega \pmod 1, \end{aligned} \tag{8}$$

which we refer to as the NK map, for which Nishikawa and Kaneko [15] proposed the fractalization route. These authors analyzed the attractor for $a = 3.0$, using ε as control parameter, computing λ (see Figure 1) and the fractal dimension. Even if they reach the conclusion that the torus is fractal (a SNA) for $0.1553 < \varepsilon < 0.1573$, they do not exclude the possibility that the fractal nature disappears at much finer scales. This is the computation that we have done, for several ε in this region. The reported results correspond to $\varepsilon = 0.157$, close to the breakdown. We observe in Figure 2 that the torus reveals its smoothness at the scale 10^{-13}, and Figure 3 shows that the maximal slope is $\geq 2.2 \times 10^{13}$.

The second example is a *qp forced Hénon map*,

$$\begin{aligned} x_{n+1} &= 1 + y_n - a x_n^2 + \varepsilon \cos(2\pi\theta_n), \quad y_{n+1} = b x_n, \\ \theta_{n+1} &= \theta_n + \omega \pmod 1, \end{aligned} \tag{9}$$

where a, b are the parameters of the Hénon map and ε leads to a qp forcing. This model, which we refer to as the RH map (from *rotating Hénon map*), is also expected to be the scenario of creation of SNAs through the fractalization route since the work of Sosnovtseva et al. [16] (see also [20, 21]). For instance, in [16] it is claimed that a SNA exists for $a = 0.7$, $b = 0.1$ and $\varepsilon = 0.7$, but Figure 4 shows that it is nonstrange at the scale 10^{-26} [32]. The maximal slope is $\geq 2.2 \times 10^{28}$.

The third example is a *qp driven logistic map*

$$\begin{aligned} x_{n+1} &= a(1+\varepsilon\cos(2\pi\theta_n))x_n(1-x_n), \\ \theta_{n+1} &= \theta_n + \omega \pmod 1. \end{aligned} \tag{10}$$

This model, which we refer to as the HH map, was introduced by Heagy and Hammel [22] to explain a *collision mechanism* of formation of SNAs, in which two 1D tori collide [33]. Prasad et al. [4, 23] proposed also the fractalization route, that is what we analyze here. We select $\varepsilon = 0.1$ and keep a as a control parameter. Figure 5 shows λ as a function of a and $\mathcal{A}$ for $a = 3.271, 3.272, 3.275$. Before $a = 3.271$ and shortly after it, the attractor is clearly an invariant curve, despite the oscillations are not so small. For $a = 3.272$ and $a = 3.275$ *it does not look* an invariant curve. But we obtain $\lambda \approx -0.00946$ and $\lambda \approx 0.00089$, respectively. It is clear that one must understand the difference between these two cases.

To analyze the fine structure of $\mathcal{A}$ for $a = 3.252$, we have applied zooms with $s = 2$, $q = 2000$ ($p = 4000$), transient $m = 10000$ and MP-77 to compute the points on $\mathcal{A}$ [12]. In particular we see that the oscillation is small for $k = 73$. The shape of $\mathcal{A}$ after these 73 halvings is displayed in Figure 6. The width of the current interval is $2^{-73} \approx 10^{-22}$. The computation has been checked for this interval using also MP-96 without observing differences. It also follows that the maximal slope of the curve is $\geq 6.3 \times 10^{21}$ (see Figure 6).

In these three examples in which fractalization was proposed as a mechanism of formation of SNAs, the attractors are really nonstrange. The phenomenon deserves an explanation, that we propose in next lines, based on the properties of the linearization of the dynamics around an invariant torus.

For $\mathcal{T}$, an invariant torus $X = X_{a,\varepsilon}(\theta)$ of (1), we consider the linear qp system

$$v_{n+1} = M_{a,\varepsilon}(\theta_n)v_n, \quad \theta_{n+1} = \theta_n + \omega \pmod 1, \tag{11}$$

where $M(\theta) = \mathrm{D}_x f(X(\theta), \theta)$. The *variational equations* (11) give the growth of perturbations v_0 transversal to $\mathcal{T}$. It is an attractor if the spectrum Spec $\mathcal{M}$ of the transfer operator $\mathcal{M}$ acting on continuous vector fields $\boldsymbol{v} : \mathbb{T} \to \mathbb{R}^n$ by

$$(\mathcal{M}\ \boldsymbol{v})(\theta) = M(\theta-\omega)\boldsymbol{v}(\theta-\omega) \tag{12}$$

is inside the unit circle (the "eigenvalues" have modulus smaller than 1).

Spec $\mathcal{M}$ is a set of annuli centred in the origin [24, 25]. For non-invertible examples 1 and 3, it is either a circle (if $M(\theta) \neq 0$ for all θ) or a disk (if $M(\theta_0) = 0$ for some θ_0). For invertible example

2 it is either two circles or a full annulus (it could be also one circle, but not in the present case). In any case, the spectral radius is given by the exponential of the maximal Lyapunov exponent λ.

When varying the parameters, if the spectral radius crosses 1 (λ crosses 0), a bifurcation is expected. In "regular" bifurcations of tori (like saddle-node, transcritical, period doubling, etc.), the spectral component that crosses 1 is a circle. In the "strange" bifurcations encountered here, Spec $\mathcal{M}$ is either a disk (examples 1 and 3 – see [13]) or a full annulus (example 2 – see [26]). Having 1 in the interior of Spec $\mathcal{M}$ is not compatible with the persistence of $\mathcal{T}$ under perturbations [27]: we cannot apply Implicit Function Theorem to the invariance equation (4) or, in other words, we can not apply Newton method to solve (4). This would explain why $\mathcal{T}$ is destroyed.

The analytical discussion above can be translated into more geometrical terms. Notice that while in "regular" bifurcations the torus, even if it can be destroyed, does not wrinkles, in the "strange" bifurcations the slopes of the torus go to infinity. So, from a geometrical point of view "regular" and "strange" bifurcations are different. The geometrical mechanism suggested by our experiments is that tangential directions to $\mathcal{T}$ merge with transversal ones (in the x-direction) [34]. At this point $\mathcal{T}$ loses normal hyperbolicity [35] and it is destroyed, leaving behind possibly a SCA. This transition deserves further study.

Acknowledgements. We thank R. de la Llave for encouragement and discussion.

* A.H. supported by MCyT Grant BFM2003-07521-C02-01. C.S. supported by MCyT Grant BFM2003-09504-C02-01. Both supported by CIRIT 2001 SGR-70 and 2005 SGR-1028.

[1] D. Ruelle and F. Takens, Comm. Math. Phys. **20**, 167 (1971).

[2] J.-P. Eckmann and D. Ruelle, Rev. Modern Phys. **57**, 617 (1985).

[3] C. Grebogi, E. Ott, S. Pelikan, and J. A. Yorke, Phys. D **13**, 261 (1984).

[4] A. Prasad, S. S. Negi, and R. Ramaswamy, Internat. J. Bifur. Chaos Appl. Sci. Engrg. **11**, 291 (2001).

[5] G. Keller, Fund. Math. **151**, 139 (1996).

[6] Z. I. Bezhaeva and V. I. Oseledets, Funktsional. Anal. i Prilozhen. **30**, 1 (1996).

[7] B. R. Hunt and E. Ott, Phys. Rev. Let. **87**, 254101 (2001).

[8] P. Glendinning, Dyn. Syst. **17**, 287 (2002).

[9] J. Stark, Dyn. Syst. **18**, 351 (2003).

[10] T. H. Jäger, Nonlinearity **16**, 1239 (2003).

[11] A. Haro and J. Puig, arXiv nlin.CD/0510073 (2005).

[12] H. Broer, C. Sim´o, and R. Vitolo, mp_arc # 05-107 (2005).

[13] A. Jorba and J. C. Tatjer, mp_arc # 05-429 (2005).

[14] A. Haro and R. de la Llave, in the SIAM Conf. on Applications of Dynamical Systems (Snowbird, UT (May 22-26, 2005).

[15] T. Nishikawa and K. Kaneko, Phys. Rev. E **54**, 6614 (1996).

[16] O. Sosnovtseva, U. Feudel, J. Kurths, and A. Pikovsky, Phys. Lett. A **218**, 255 (1996).

[17] J. Stark, Phys. D **109**, 163 (1997), physics and dynamics between chaos, order, and noise (Berlin, 1996).

[18] A. Haro and R. de la Llave, J. Differential Equations (to appear).

[19] C. Sim´o, in Proceedings Equadiff03, ed. F. Dumortier et al., World Scientifi c, pp. 631–636 (2005).

[20] S.-Y. Kim and W. Lim, J. Phys. A **37**, 6477 (2004).

[21] A. Y. Jalnine and A. H. Osbaldestin, Phys. Rev. E (3) **71**, 016206, 14 (2005).

[22] J. F. Heagy and S. M. Hammel, Phys. D **70**, 140 (1994).

[23] A. Prasad, V. Mehra, and R. Ramaswamy, Phys. Rev. Let. **79**, 4127 (1997).

[24] J. N. Mather, Nederl. Akad. Wetensch. Proc. Ser. A 71 = Indag. Math. **30**, 479 (1968).

[25] A. Haro and R. de la Llave, Preprint (2003).

[26] A. Haro and R. de la Llave, Chaos (to appear).

[27] R. Mañ´e, Trans. Amer. Math. Soc. **246**, 261 (1978).

[28] A. Haro and R. de la Llave, mp_arc # 05-246 (2005).

[29] M. Hirsch, C. Pugh, and M. Shub, *Invariant manifolds* (Springer-Verlag, Berlin, 1977), lecture Notes in Mathematics, Vol. 583.

[30] In the literature, most of the models in which SNAs appear (or seem to appear), are qp forced dynamical systems. Notice, however, that the mechanism of formation of SNAs in [11, 26] works in a more general setting, not just for qp systems

[31] Since the limit (2) does not always exist, one can replace $\lim$ by $\limsup$ in (2).

[32] Other studies [26, 28] suggest that SNAs do not appear in the nonlinear dynamics, but in the linear dynamics around invariant tori (see also [21]). This linear behavior is the prelude of the destruction of the regular motion in the nonlinear dynamics.

[33] Notably, the collision mechanism has been proved rigorously in [5, 6, 10] in several cases. It is also the mechanism of formation on SNA in Harper maps [11], projectivizations of 2D qp linear maps [26].

[34] For mechanisms in which two different invariant transversal directions merge, see [26].

[35] There are two conditions for normal hyperbolicity [29]. A geometrical one: for the tangential directions to $\mathcal{T}$ one can construct complementary invariant transversal –normal– directions. And a dynamical one: the dynamics on the transversal directions is "hyperbolic" and "dominates" the tangential dynamics. If λ comes to zero in the transversal directions, a bifurcation is produced because the dynamical condition fails. Notice, however, that in "regular" bifurcations the geometrical condition holds, while in "strange" ones it fails.

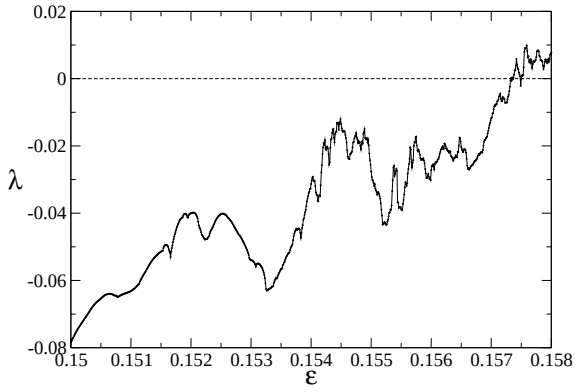

Figure 1: The Lyapunov exponent of the attractor as a function of ε, for the NK map with $a = 3.0$.

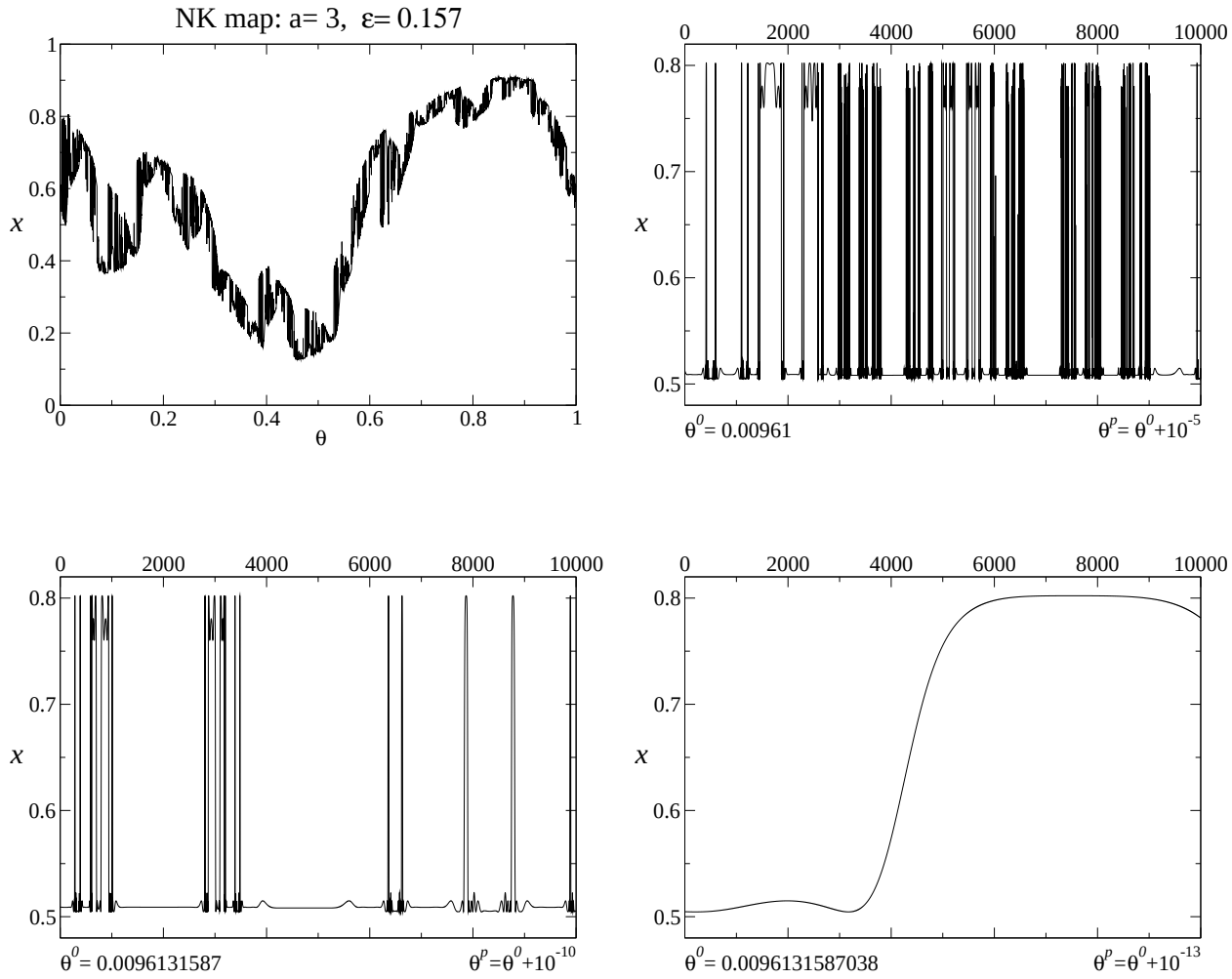

Figure 2: The attractor of the NK map with $a = 3.0$,$\varepsilon = 0.157$, and several zooms using $s = 10$, $q = 10^3$ ($p = 10^4$). We found $\lambda \approx -0.01173$, and *mpols* $P \approx 32$. The plots show the corresponding "broken lines" for $k = 0, 5, 10, 13$. To compute $\mathcal{A}$, we have used $m = 20000$ and MP-57. The estimated precision is $d_r \approx 37$.

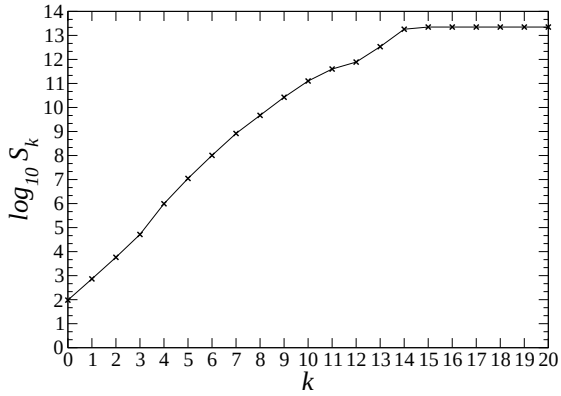

Figure 3: Averaged slope S_k, in $\log_{10}$ scale, as a function of k with s, q as before. The variation at step k is $V_k = 10^{-k} S_k$.

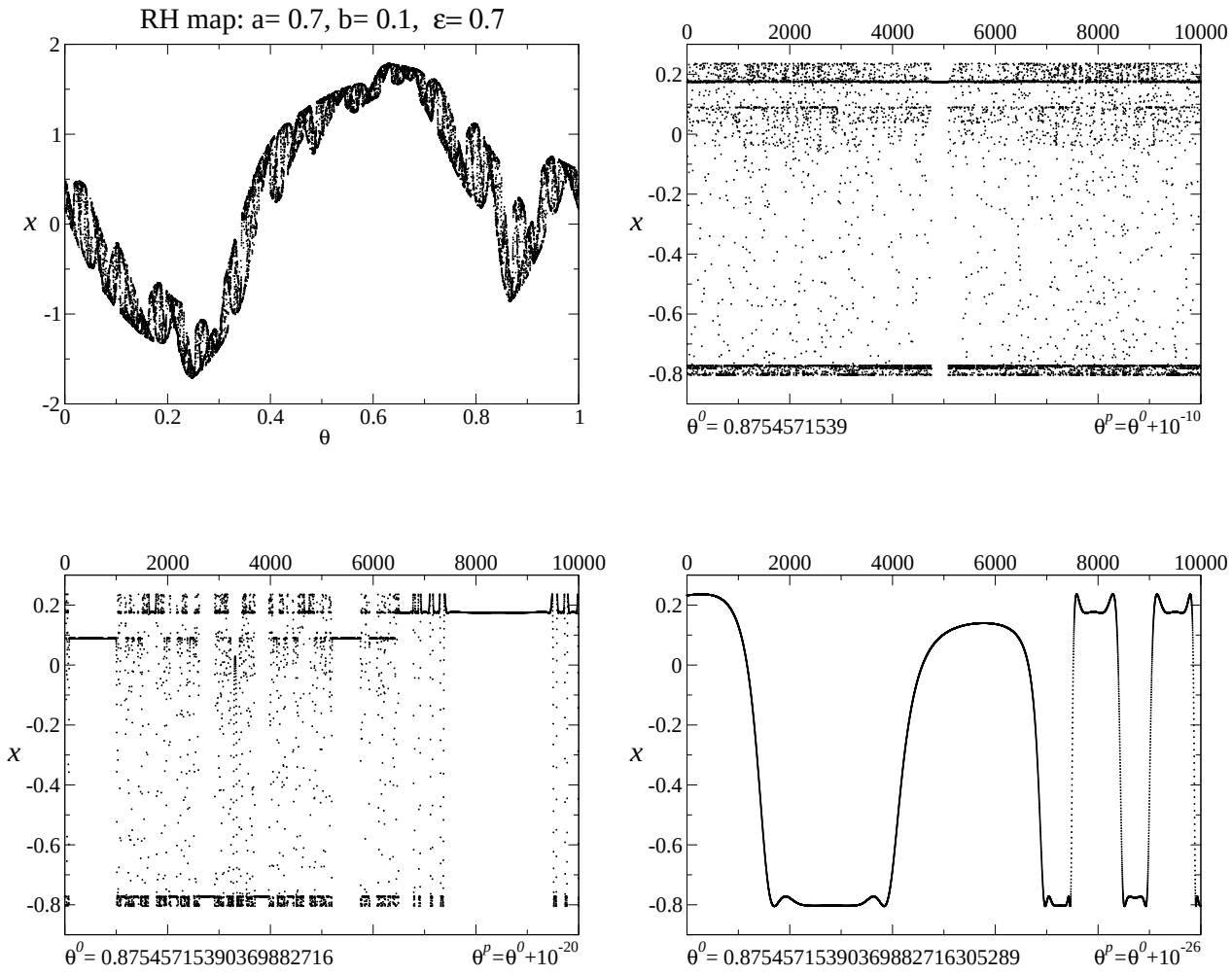

Figure 4: The attractor of the RH map with $a = 0.7$, $b = 0.1$ and $\varepsilon = 0.7$, and several zooms using $s = 10, p = 1000$. We found $\lambda \approx -0.00361$, and *mpols* $P \approx 46$. The plots show the corresponding "dust of points" for $k = 0, 10, 20, 26$. To compute $\mathcal{A}$, we have used $m = 50000$ and MP-77. Estimated precision $d_r \approx 57$.

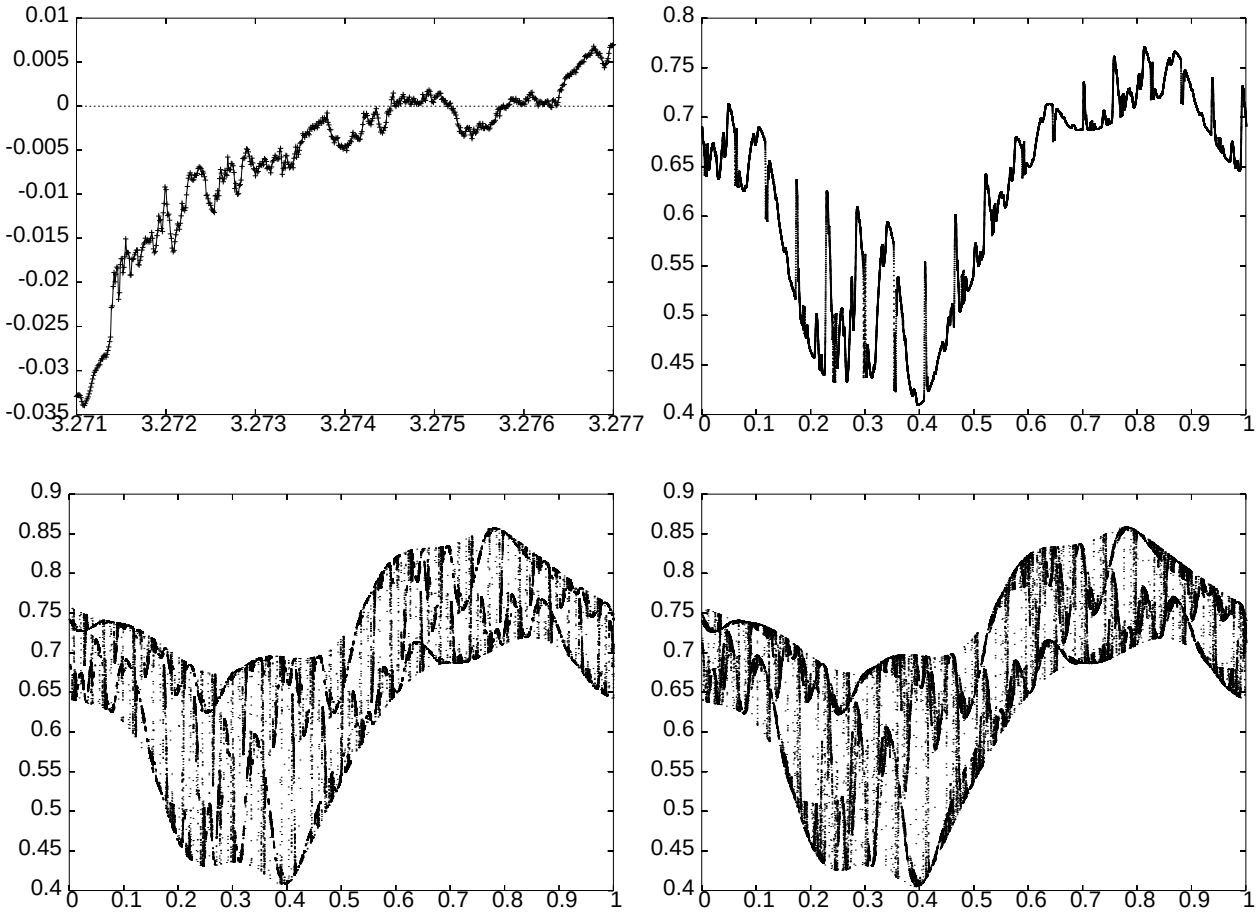

Figure 5: Top left: The Lyapunov exponent of the attractor as a function of a, for the HH map with $\varepsilon = 0.1$. Top right and bottom: The attractor of the HH map with $\varepsilon = 0.1$, for $a = 3.271, 3.272, 3.275$.

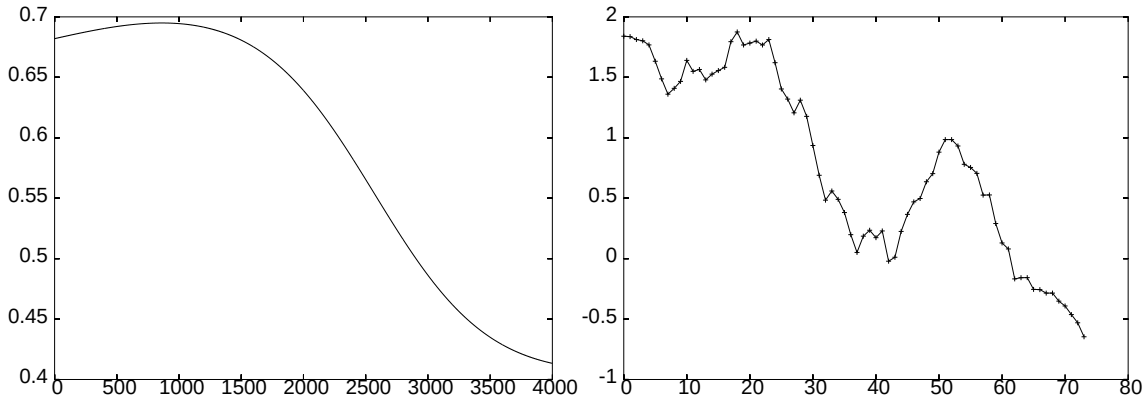

Figure 6: HH map for $\varepsilon = 0.1$ and $a = 3.252$. Left: the attractor after 73 halvings. The interval is $0.391619055959714067756 + 10^{-21} \times [0.6728242712, 0.7787033896]$. Right: The local variation V_k, in $\log_{10}$ scale, at each step k of the zooms, with $s = 2$, $q = 2000$ ($p = 4000$). The averaged slope at the step k is $S_k = 2^k V_k$.